This article was downloaded by:[Univ of California Library]
[Univ of California Library]
On: 21 May 2007
Access Details: [subscription number 769844339]
Publisher: Taylor & Francis
Informa Ltd Registered in England and Wales Registered Number: 1072954
Registered office: Mortimer House, 37-41 Mortimer Street, London W1T 3JH, UK

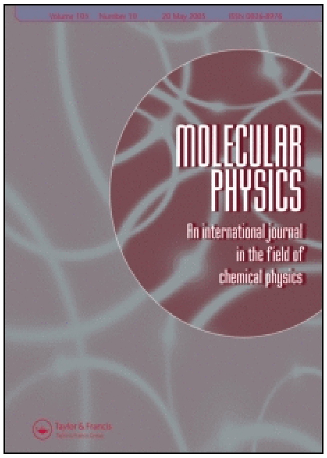

Molecular Physics

An International Journal in the Field of Chemical Physics

Publication details, including instructions for authors and subscription information:
http://www.informaworld.com/smpp/title~content=t713395160

Refinements in the description of excited VRT states of the water dimer

To cite this Article: Harker, H. A., Keutsch, F. N., Leforestier, C., Scribano, Y., Han, J.-X. and Saykally, R. J. , 'Refinements in the description of excited VRT states of the water dimer', Molecular Physics, 105:5, 513 - 527
To link to this article: DOI: 10.1080/00268970601153373
URL: http://dx.doi.org/10.1080/00268970601153373

PLEASE SCROLL DOWN FOR ARTICLE

Full terms and conditions of use: http://www.informaworld.com/terms-and-conditions-of-access.pdf

This article maybe used for research, teaching and private study purposes. Any substantial or systematic reproduction, re-distribution, re-selling, loan or sub-licensing, systematic supply or distribution in any form to anyone is expressly forbidden.

The publisher does not give any warranty express or implied or make any representation that the contents will be complete or accurate or up to date. The accuracy of any instructions, formulae and drug doses should be independently verified with primary sources. The publisher shall not be liable for any loss, actions, claims, proceedings, demand or costs or damages whatsoever or howsoever caused arising directly or indirectly in connection with or arising out of the use of this material.

© Taylor and Francis 2007

Molecular Physics, Vol. 105, No. 5–7, 10 March–10 April 2007, 513–527

Taylor & Francis
Taylor & Francis Group

Refinements in the description of excited VRT states of the water dimer

H. A. HARKER†, F. N. KEUTSCH‡, C. LEFORESTIER§,
Y. SCRIBANO§, J.-X. HAN† and R. J. SAYKALLY*†
†University of California, Berkeley, USA
‡University of Wisconsin, Madison, USA
§Université de Montpellier II, Montpellier, France

(*Received 5 September 2006; accepted 5 December 2006*)

Extensive new spectroscopic measurements are combined with a global analysis of the ground state data in order to re-examine and to refine the description of the excited vibration rotation tunneling (VRT) states of the water dimer. Notably, six new 'donor torsion' subbands are analytically identified, current vibrational assignments of the $K_a = 1$ stacks are reassessed, the previously reported $(H_2O)_2$ donor torsion overtone $(DT)^2$ and hydrogen bond stretch (S) data sets are augmented, and four new (S) subbands have been measured. Unusually large Coriolis effects are predicted, excited state $E_2 \leftrightarrow E_1$ assignments are reinforced, and possibilities of experimentally determining ground state AS splitting in $(H_2O)_2$ from excited state data are discussed.

1. Introduction

Spectroscopic studies of the intermolecular vibrations of small water clusters have produced highly detailed structural and dynamical information that has permitted the determination of a new generation of 'first principles' potential energy surfaces (PES) for water [1, 2]. Studies of the water dimer are of particular significance given the primarily two-body nature of the PES along with the rapid convergence of the remaining non-additive terms. Hence, it is crucial to seek a 'perfect' dimer intermolecular potential energy surface (IPS).

Here, compiled water dimer ground state transitions recently reported by Harker *et al*. [3] are used to refine the description of the excited VRT states of the water dimer. We demonstrate the efficacy of global fitting via the identification and analysis of all six asymmetry components of a new 'DT' band. Furthermore, we describe how this analysis has led to a reassessment of the vibrational assignments within the $K_a = 1$ stacks of both $(H_2O)_2$ and $(D_2O)_2$. Third, we extend and clarify existing analyses of the $(H_2O)_2$ donor torsion overtone $(DT)^2$ and the hydrogen bond stretch (S) [4] by augmenting existing subbands as well as by identifying and assigning four new S subbands. We demonstrate that Coriolis effects of unprecedented magnitude are expected in this spectral region. Lastly, we assess the proposal by Keutsch *et al*. [4] that E_1 $(K_a = 0) \leftarrow E_2$ $(K_a = 1)$ have been observed in the vibrationally excited H_2O water dimer. We also propose an alternative means of determining the $(H_2O)_2$ ground state AS splittings, namely from excited state data.

2. Background

Previous studies indicate that the water dimer is a highly nonrigid, near-prolate top that simultaneously undergoes three large amplitude tunneling motions [5–12]. Tunneling occurs among eight degenerate minima on the 12D IPS (6D for rigid potentials) via the three low barrier pathways [13, 14] splitting the rovibrational levels [6, 10, 12]. The lowest barrier motion, acceptor switching (AS), effectively splits each rovibrational level into two labelled A_1/B_1 or A_2/B_2, while the interchange (I) and bifurcation tunneling (BT) motions further split/shift these two levels into two sets of three. The six resulting energy levels remain grouped into two sets according to the original AS splitting and are henceforth referred to as the 1s and the 2s. The 1s comprise the states $A_1^+/E_1^+/B_1^+$ whereas the 2s comprise $A_2^-/E_2^-/B_2^-$.

---

*Corresponding author. Email: saykally@calmail.berkeley.edu

ISSN 0026–8976 print/ISSN 1362–3028 online © 2007 Taylor & Francis
http://www.tandf.co.uk/journals
DOI: 10.1080/00268970601153373

It is crucial to note that the numeric label for the doubly degenerate E states is purely one of convenience and does not affect the selection rules as does that of the A and B states: $A_1^+ \leftrightarrow A_1^-$, $A_2^+ \leftrightarrow A_2^-$, $B_1^+ \leftrightarrow B_1^-$, $B_2^+ \leftrightarrow B_2^-$, $E^+ \leftrightarrow E^-$ [6]. Transitions among A and B states are therefore only allowed within a given set, while transitions among E states transcend this restriction.

In order to establish the nomenclature for the spectroscopic analysis that follows, we also briefly review some salient features of the vibrationally excited water dimer VRT states. Reimer and Watts (R&W) performed a normal mode analysis on their RWK2 intermolecular potential energy surface (IPS) [15] and found 12 normal modes for the vibrationally excited water dimer, six of which correspond to the intermolecular vibrations that are of interest here; the other six correspond to intramolecular vibrations. The six intermolecular modes are shown in figure 1, with the labels of R&W. Obviously, such a normal mode analysis is poorly suited to the water dimer, given its large amplitude vibrations. Recently, Leforestier *et al.* [16] and Smit *et al.* [17] carefully analysed the nodal patterns of the vibrational wave functions derived from the SAPT-5st and VRT(MCY-5f) IPS respectively. They showed that combination and vibrational overtone bands need to be considered and that the ordering of vibrational symmetries differed not only from the harmonic ordering, but also between the $K_a = 0$ and 1 stacks. Theoretical calculations presently agree well on the ordering of the vibrational and tunneling levels, so that differences in vibrational assignments remain only in the labelling. We have subsequently adopted the labeling scheme of Smit *et al.* in accord with the work of Keutsch *et al.* [4] for intermolecular vibrations, as will be discussed later. The normal mode vibration labels of R&W do, however, facilitate discussion, and so are reviewed here.

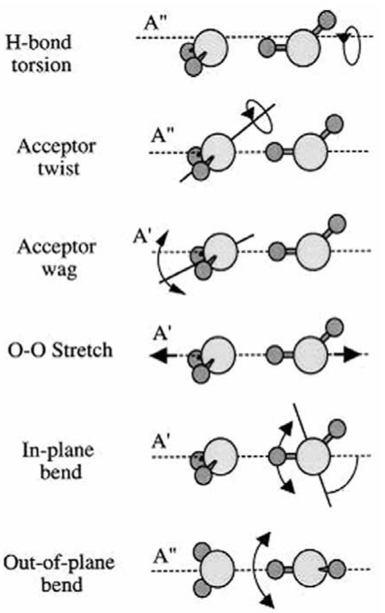

Figure 1. Six intermolecular normal modes – as determined and labelled by Reimer and Watts [15]. The H-bond torsion is interchangeably referred to as the donor torsion (DT). A″ motions occur out of the plane of symmetry of the water dimer, whereas A′ motions occur within the plane of symmetry. This affects the ordering of A″ vibrationally excited energy levels by interchanging the 1s and the 2s as well as their parity and consequently the types of allowed transitions. Notably, Q-branch ($\Delta J = 0$) transitions are not allowed in a-type $\Delta K_a = 0$ bands for vibrations of A″ symmetry.

3. Experiment

Details of the Berkeley Terahertz VRT spectrometers have been presented elsewhere [18, 19]. Furthermore, the experimental conditions concerning previously observed, lower frequency, bands presented in this work were reported at the time of their publication [11, 12]. Therefore, only details relevant to the new high frequency (4 THz) experiments will be reported here. Terahertz radiation was generated through the first-order mixing of tunable microwave radiation with the output of a fixed frequency far-infrared (FIR) molecular gas laser. The two FIR lasers used for the high frequency work were the 70 µm (4251.6736 GHz) CH_3OH and 72 µm (4158.9158 GHz) $^{13}CH_3OH$ lasers. Two microwave sources were also used: an HP8367B microwave synthesizer (fundamental, first, or second harmonic) covering frequencies from 2 to 60 GHz and a KVARZ millimetre synthesizer covering frequencies from 53 to 118 GHz. The former microwave radiation source was coupled onto the antenna of an IT24 Schottky barrier diode via direct coaxial coupling whereas the latter was free space coupled via a spherical focusing mirror. The nonlinear properties of the diode result in the generation of two tunable sidebands with frequencies of $\nu(\text{laser}) \pm \nu(\text{microwave})$. The probe signal was then separated from the residual laser radiation and multipassed in front of a 10 cm slit source, which pulses at a repetition rate of 33 Hz forcing a ~1% H_2O or D_2O in Ar mixture to adiabatically expand into a vacuum chamber maintained at 35 mTorr. The direct absorption signal was detected using an unstressed germanium/gallium photoconductive detector. The absolute accuracy of the experiment, determined by thermal laser drift, is ~3 MHz, whereas the effective resolution in the 70 µm frequency region, as a result of Doppler broadening, is ~3.9 MHz.

4. Results and discussion

4.1. $K_a = 1 \leftarrow 1$ 'DT' subbands

Close inspection of the experimentally observed $(D_2O)_2$ 'DT' bands (figure 2) yielded precise knowledge of both the $K_a = 0$ and 1 excited states that, when combined with the accurately determined ground state parameters [3], allowed us to predict, identify, and analyse all six asymmetry components corresponding to the $K_a = 1 \leftarrow 1$ band of the 2s. It should be noted that $K_a = 0 \leftarrow 0$ transitions are not allowed for A″ vibrations such as the DT. However, all $\Delta K_a = 0$ transitions are actually not forbidden for A″ vibrations. Rather, $\Delta K_a = 0$ transitions for which $\Delta J = 0$ are not allowed since this necessitates $\Delta K_c = 0$. The observation of a $\Delta K_a = 0$ band for an A″ vibration is therefore not remarkable, beyond refinement of the excited states; however, we have undeniably identified Q-branch transitions, $\Delta J = 0$, for this band which does indeed contradict the assignment of the 2s of the $K_a = 1$ stack of the 'DT' to an A″ vibration. This analysis has consequently lead to a better understanding of the $K_a = 1$ excited states of the $(D_2O)_2$ vibration that were originally assigned to the DT, but has also raised some fundamental questions.

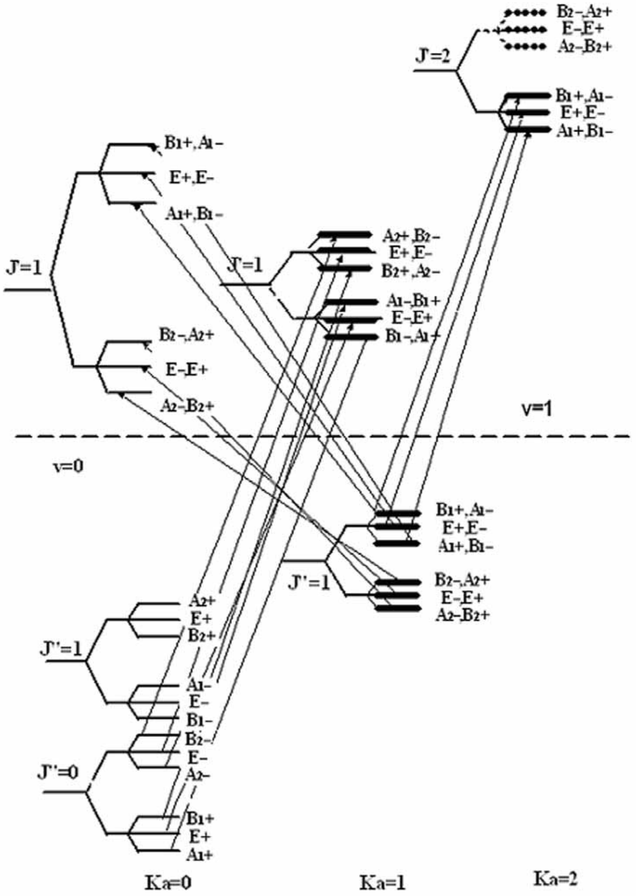

Figure 2. Previously observed $(D_2O)_2$ 'DT' bands. The observation and analysis of these bands provided detailed knowledge of the $K_a = 0$ and 1 excited states.

Allowed transitions must, in fact, be associated with at least one of the following: $\Delta J \neq 0$, $\Delta K_a \neq 0$, or $\Delta K_c \neq 0$. In the case of $\Delta K_a = 0$ transitions, either J or K_c must necessarily change. Energy level diagrams of A′ and A″ vibrations greatly facilitate understanding of the arguments that follow and are so provided in figure 3(a) and 3(b), respectively. Recalling the water dimer selection rules, inspection of the A″ correlation diagram shows that $\Delta K_a = 0$ transitions are indeed allowed, but that this forces $\Delta J \neq 0$. An example of such a transition (figure 3(b)) would be: $A_2^-(J = 2,\ K_a = 1,\ K_c = 2) \leftarrow A_2^+(J = 1,\ K_a = 1,\ K_c = 0)$. We have, however, observed $\Delta K_c = 1$, $\Delta J = 0$ transitions for the 2s of a $K_a = 1 \leftarrow 1$ band, which terminate in the same excited states as the 2s of the $K_a = 1 \leftarrow 0$ transitions assigned to the $(D_2O)_2$ DT by Braly [12]. **This is in direct contradiction with the assignment of these transitions to an A″ vibration!** These new transitions were analytically predicted using the Braly's listed excited states. The commonality of the $K_a = 1$ excited states is therefore unequivocally established, as is their A′ vibrational symmetry. The assigned transitions along with their fit residuals are listed in table 1; the fitted rotational constants and tunneling splittings are presented in table 2. The greater number of observed E-state transitions is easily attributable to the nuclear spin weights of the D_2O water dimer which are A_2^+/A_2^- (3), B_2^+/B_2^- (6), E^+/E^- (18).

Simultaneous fitting of the previously observed $(D_2O)_2$ 'DT' bands and the newly identified band unequivocally establishes the ordering of the asymmetry labels of the excited state 2s of the $K_a = 1$ stack. Indeed, the first identified c-type transitions originating in $K_a = 0$ and terminating in $K_a = 1$ could have been assigned to either the lower (A″) or the upper asymmetry component (A′) of the $K'_a = 1$ stack. Only the additional observation of these new a-type transitions locks in the asymmetry assignment of the excited state 2s of the $K_a = 1$ stack, thereby establishing their vibration type as A′. Similarly, the transitions currently assigned to the 1s of the DT $K_a = 2 \leftarrow 1$ actually belong to an A′ vibration, and therefore cannot be assigned to the DT vibration. In contrast, both the 1s and the 2s of the $K_a = 0 \leftarrow 1$ DT bands do correspond to an A″ type vibration, as evidenced by ground state combination differences. Note that combination differences alone cannot be used to determine the vibrational symmetry of transitions originating in $K_a = 0$ and terminating in $K_a > 0$. For this very reason, the 1s of the 'DT' $K_a = 1$ stack are of unconfirmed vibrational symmetry. This situation can, however, be resolved through experiment.

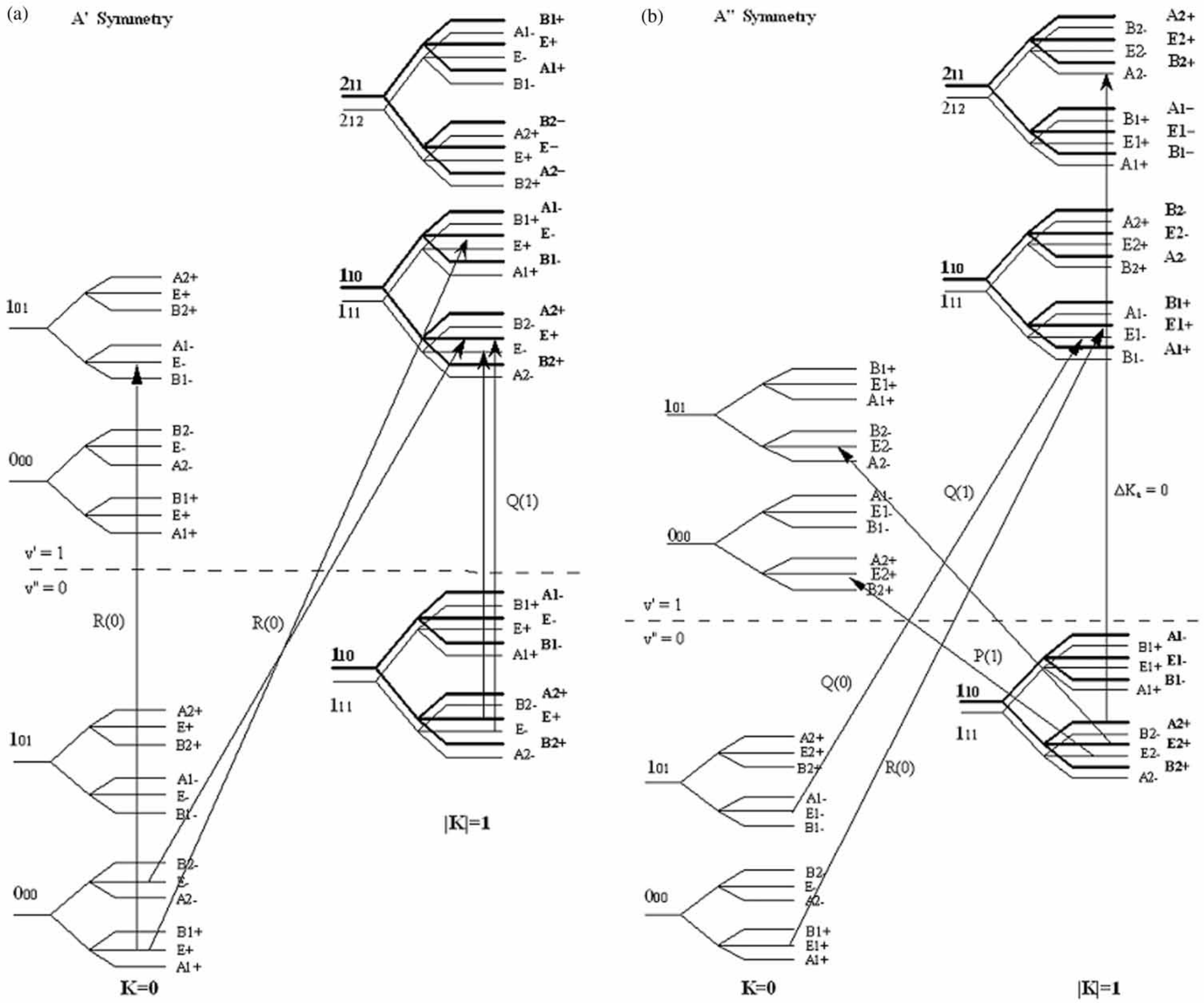

Figure 3. Correlation diagram for (a) A′ and (b) A″ symmetry vibration. States are labelled $J_{\mathrm{Ka,\ Kc}}$. The large K in bold refers to K_a. Arrows show examples of allowed transitions.

Allowed $K_a = 1 \leftarrow 1$ transitions of the 1s may be predicted and searched for under both scenarios, A′ and A″ vibration symmetry. Once they are identified, combination differences as well as the presence or lack therein of Q-branches will definitively establish their vibrational symmetry.

The same type of analysis can be applied to the $(D_2O)_2$ AW bands. While the 1s and the 2s of the $K_a = 0$ stack, as well as the 1s of the $K_a = 1$ stack, are of confirmed A′ vibrational symmetry, the symmetry of the AW 2s of the $K_a = 1$ stack cannot be confirmed. Furthermore, one of the asymmetry components of the 2s of the $K_a = 1$ stack for the AW is Coriolis-coupled to the 2s of the $K_a = 0$ stack of the AT (figure 4). Since coupling can only occur between states of identical symmetry and since the A″ vibrational nature of these AT bands can be confirmed through ground state combination differences, the lower asymmetry components of the AW 2s of the $K_a = 1$ stack will necessarily be those perturbed if they are of A′ symmetry, whereas the upper asymmetry components would be those perturbed if they are of A″ symmetry. This nuance becomes important when predicting the $K_a = 1 \leftarrow 1$ transitions for the AW that will allow definitive assignment of a vibrational symmetry to the 2s.

To summarize, two sets of $K_a = 1$ energy levels remain unconfirmed as to vibrational symmetry in the current $(D_2O)_2$ data set: the 1s previously assigned to the DT and the 2s previously assigned to the AW. Additionally, the 2s of the $K_a = 1$ stack that were previously assigned

Table 1. New $(D_2O)_2$ 'DT' transitions (MHz).

$K_a = 1 \leftarrow 1$									
		A_2^-/B_2^+	o–c		E_2^-/E_2^+	o–c		B_2^-/A_2^+	o–c
P4	B_2^+	1971526.99	−0.33						
P3	A_2^-	1982396.92	−0.05	E_2^-	1978064.92	−0.86	B_2^-	1973731.9	−0.36
P2				E_2^+	1988912.3	−2			
Q4				E_2^+	2010866.16	2.11			
Q3				E_2^-	2010752.4	−0.75			
Q2				E_2^+	2010669.3	0.09			
Q1				E_2^-	2010612.5	−0.97			
R1				E_2^-	2032216.2	−0.82			
R2	B_2^+	2047333	−1.05	E_2^+	2043014	−1.39			
R3	A_2^-	2058103.4	1.5	E_2^-	2053800.2	−0.55	B_2^-	2049497.52	−1.9
R4	B_2^+	2068851.3	−0.04	E_2^+	2064571.5	−0.41	A_2^+	2060291	−0.72
R5				E_2^-	2075327.9	0.33			
R6	B_2^+	2090290.7	0.41	E_2^+	2086065	−1.38			
R7				E_2^-	2096787.6	0.71			
		B_2^+/A_2^-	o–c		E_2^+/E_2^-	o–c		A_2^+/B_2^-	o–c
P4	A_2^-	1971163.39	3.67						
P3	B_2^+	1982152.3	−0.9	E_2^+	1977821.47	−0.77	A_2^+	1973488.93	−0.533
Q1	B_2^+	2014856.36	−0.16	E_2^+	2010515	−1.14	A_2^+	2006169.44	−2.43
R1				E_2^+	2032271.3	0.26			
R2				E_2^-	2043065.84	1.73	B_2^-	2038745.2	1.28
R3	B_2^+	2058126.2	−0.66	E_2^+	2053824.4	1.54	A_2^+	2049520.8	−0.87
R4				E_2^-	2064547.6	1.24	B_2^-	2060266.3	−1.39
R5				E_2^+	2075232	−1.63			

Asymmetry label pertains to the ground state.
o–c is the difference between the observed and the calculated transition frequency.

Table 2. Rotational constants and tunneling splittings of the $(D_2O)_2$ DT (MHz).

		B_1^-/A_1^+	E_1^-/E_1^+	A_1^-/B_1^+	B_2^+/A_2^-	E_+^-/E_2^-	A_2^+/B_2^-
$K'_a = 0$	$B^{(0)}$	5460.4 (1)	5457.29 (6)	5454.3 (1)	5402.12 (9)	5400.4 (2)	5398.7 (1)
	$D^{(0)}$	0.053 (2)	0.0507 (6)	0.515 (3)	0.038 (1)	0.036 (3)	0.038 (2)
	$\nu^{(0)}$		2 194 544.1 (8)			1 733 390.2 (9)	
	$I^{(0)}$		9838 (2)			6094 (2)	
	$\nu_{BT}^{(0)}$		−18.5 (8)			−5.5 (9)	
		A_1^+/B_1^-	E_1^+/E_1^-	B_1^+/A_1^-	A_2^-/B_2^+	E_2^-/E_2^+	B_2^-/A_2^+
$K'_a = 1$	$B^{(1)}$	5367.85 (6)	5367.37 (5)	5367.07 (5)	5422.5 (2)	5420.16 (6)	5418.1 (2)
	$D^{(1)}$	0.0286 (8)	0.0281 (6)	0.0287 (5)	0.046 (4)	0.040 (1)	0.04 (1)
	$(B-C)^{(1)}/4$	14.74 (4)	14.90 (3)	15.09 (3)	9.56 (8)	9.57 (4)	9.66 (2)
	$d^{(1)}$	0.0015 (7)	0.0009 (4)	0.0007 (4)	−0.003 (3)	−0.0011 (8)	−0.006 (9)
	$\nu^{(1)}$		1 981 398.5 (6)			2 099 724.4 (6)	
	$I^{(1)}$		3951 (1)			7697 (2)	
	$\nu_{BT}^{(1)}$		5.6 (6)			−6.3 (6)	

to the DT have been shown of A′ symmetry, and must consequently be reassigned to another vibration. Lastly, the 1s of the $K_a = 1$ stack that are currently assigned to the AW are of A′ symmetry. We now examine the current theoretical understanding of the D_2O water dimer.

$K_a = 0$ investigations of the D_2O dimer have been reported only for the SAPT-5st [17] and VRT(ASP-W)III [20] potentials, while $K_a = 1$ investigations are restricted to the SAPT-5st potential alone. SAPT-5st and VRT(ASP-W)III agree on the energetic ordering of A′ and A″ vibrations for the $K_a = 0$ stack.

This ordering, along with that proposed for the $K_a = 1$ stack using SAPT-5st, is listed in table 3. Since we do not question the vibrational symmetry assignments pertaining to the $(D_2O)_2$ $K_a = 0$ stack, we can confidently assert that theory agrees quite well with experimental ordering of vibrational symmetries for this stack. For the $K_a = 1$ stack, table 3 shows that the three lowest energy $K_a = 1$ vibrations in $(D_2O)_2$ are predicted as A″, A′, and A′ in contrast with the $K_a = 0$ stack where the ordering is A″, A′, A″.

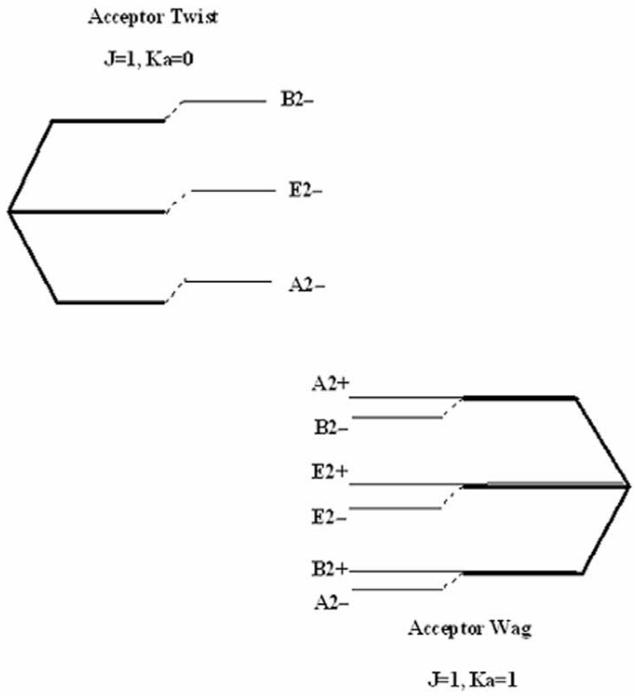

Figure 4. Coriolis coupling of the acceptor twist and acceptor WAG energy levels. The AT is of confirmed A″ symmetry; the AW energy levels shown here are of A′ vibrational symmetry.

We stress that the vibrational levels of the $K_a = 1$ stack have modal characters predicted to differ substantially from those of the nearby $K_a = 0$ levels. Nonetheless, the $K_a = 1$ stacks have traditionally been assigned to vibrational modes based on their proximity to $K_a = 0$ levels and often without confirmation of their vibrational symmetry. Table 4 lists the band origins of the 1s and the 2s for each of the three lowest energy $(D_2O)_2$ vibrations of $K_a = 0$ as well as for the four $K_a = 1$ $(D_2O)_2$ bands. We note, for example, that one could well assign the $70.0\,\mathrm{cm}^{-1}$ 2s (Braly 'DT') and the $83.3\,\mathrm{cm}^{-1}$ 1s (Braly 'AW'), which are both of confirmed A′ symmetry, to the AW vibration. This would resolve the long-standing AW dilemma; the 2s have been thought higher in energy than the 1s in contradiction with the energy correlation diagram of an A′ vibrational symmetry. Therefore the vibrational assignments of all $K_a = 1$ energy levels, both for the H_2O and D_2O dimer, should be revisited. In particular, $K_a = 1 \leftarrow 1$ transitions should be predicted for all $K_a = 1$ levels of unconfirmed symmetry, assuming both an A′ and an A″ vibration, and current databases searched for the relevant transitions. If this fails, additional experimental searches should be performed. We remark also that the difficulties associated with vibrational assignments will be compounded in the case of $(H_2O)_2$ since no vibrational transitions have ever been observed that originate in the 1s of the $K_a = 1$ stack, presumably because of low thermal populations. Until the vibrational symmetries of $K_a = 1$ levels are confirmed, it is not reasonable to associate them with any particular

Table 3. Energies of $(D_2O)_2$ states from SAPT-5st (cm^{-1}).

	State (J, K, v)[b]	C_s irrep	Energy	Mode
$J = K = 0$	(0,0,0)	A′	0	GS
	(0,0,1)	A″	67.35	DT
	(0,0,2)	A′	91.58	AW
	(0,0,3)	A″	92.04	AT
	(0,0,4)	A′	123.07	$(DT)^2$
	(0,0,5)	A′	146.82	S
	(0,0,6)	A″	146.06	DT + AW
$J = \|K\| = 1$	(1,1,0)	A′	3.96	GS
	(1,1,1)	A″	69.68	DT
	(1,1,2)	A′	93.18	AW
	(1,1,3)	A′	100.79	$(DT)^{2\,a}$
	(1,1,4)	A″	122.61	DT + AW
	(1,1,5)	A′	146.15	S

[a] Assignment of this mode from its nodal character is uncertain.
[b] vth state with total angular momentum J and projection number K.

Table 4. Experimentally determined $(D_2O)_2$ band origins (cm^{-1}).

$K_a = 0$			$K_a = 1$			
DT	1s	73.2	"DT"	1s	66.0	A′ or A″
	2s	57.8		2s	70.0	A′
AW	1s	80.4	"AW"	1s	83.3	A′
	2s	82.6		2s	87.7	A′ or A″
AT	1s	**90.7				
	2s	88.5				

**Not exact due to a non-observed subband.For comparison with table 3, add $AS^{(0)} = 2.2\,cm^{-1}$ to each value of the 2s, so as to account for different zero-energy reference points, then average the value of the 1s and the 2s. Example $K_a = 0$ DT: ((57.8+2.2) + 73.2) = $66.6\,cm^{-1} \sim 67.35\,cm^{-1}$.

vibrational mode. We add that the theoretical predictions of Smit *et al.* coincide well with the experimental results for the $K_a = 0$ stack and that these predictions should aid in the vibrational assignments of the $K_a = 1$ levels once their vibrational symmetries have been established.

4.2. *$(H_2O)_2$ donor torsion overtone $(DT)^2$ and the hydrogen bond stretch (S)*

While vibrational symmetries and modal assignments of $(H_2O)_2$ bands are determined using all of the same types of arguments as presented in section 4.1, two additional features become important for the non-deuterated water dimer. First, as explained in the previous section, states with the same overall symmetry and same *J* rotational quantum number may perturb each other. In the vibrational ground state of the H_2O water dimer, the 2s of the $K_a = 0$ stack are sufficiently close in energy to the upper asymmetry component of the 2s of the $K_a = 1$ stack for Coriolis coupling to occur. This Coriolis perturbation results in characteristic frequency shifts of all transitions involving the affected ground states. Second, the relative intensities of transitions are determined by nuclear spin weights as follows for $(D_2O)_2/(H_2O)_2$: $A_1^{\pm}$ (21/1), $A_2^{\pm}$ (3/3), $B_1^{\pm}$ (15/0), $B_2^{\pm}$ (6/6), $E^{\pm}$ (18/3). Of particular note, the nuclear spin weight of $B_1^{\pm}$ transitions is null in $(H_2O)_2$. Therefore, in the A_1^+/B_1^- and A_1^+/B_1^- bands, every other line is missing. While this characteristic fingerprint aids identification, it also leads to sparser spectra. Furthermore, enhanced tunneling splittings in the H_2O water dimer compared to the D_2O dimer already lead to expansive H_2O water dimer spectra, so much so that frequently more than one FIR laser is needed in order to fully characterize a given intermolecular vibration. These types of factors make the H_2O water dimer more difficult to assign than its perdeuterated counterpart, while at the same time providing for less ambiguous assignments.

Recently, Keutsch *et al.* described several bands assigned to the $(H_2O)_2$ donor torsion overtone $(DT)^2$ and the stretch (S) [4], as per the mode labelling of Smit *et al.* [17]. Since then, the number of assigned transitions associated with these vibrational modes has almost tripled, in large part through the addition of previously unobserved bands. Here, we review and refine this analysis at the same time that we present these new transitions. Table 5(a) lists both the new transitions (bold) and those previously assigned by Keutsch *et al.* Table 5(b) lists the molecular constants determined in the fits using the equations given in [4].

Arguments similar to those presented in the last section were used to confirm the ground and excited state K_a stacks of the A and B subbands listed in tables 5(a) and (b). Additionally, Keutsch *et al.* [4] also reasoned that the observed P(1) transition at 4296051.5 MHz, associated with a subband devoid of Q-branch transitions could only be consistent with a $K_a = 0 \leftarrow 0$ assignment, whereas the subbands lacking R(0) transitions but terminating in the same excited states as the former required a $K_a = 0 \leftarrow 1$ assignment. Assignment of the A and B subbands were therefore unequivocally established. In contrast, assignment of the 4261 GHz E-state transitions, while consistent with a $K_a = 0 \leftarrow 1$ assignment, could not be confirmed. Since then, we have predicted analytically the $K_a = 0 \leftarrow 0$ E_2^-/E_2^+ transitions that would be expected given this assignment, and no matches were found, which is quite troublesome. Furthermore, the expected P(1) transition that would allow us to confirm this assignment is unfortunately located in a gap of the current scanning range of the spectrometer. Keutsch *et al.* [4] originally assigned the 4261 GHz E_2 transitions to the $K_a = 0 \leftarrow 1$ subband for two reasons: (1) ground state combination differences showed that they originated in the lower asymmetry components of the $K_a = 1$ stack and (2) the only other observed E subband was located much higher in frequency at 4295 GHz effectively located outside of the 2s fork of the $K_a = 0$ stack as defined by the

Table 5(a). $K_a = 0$ (DT)^2 bands and $K_a = 1$ (S) bands of $(H_2O)_2$ (MHz).

Transition	Frequency	A_2^-/B_2^+	Δ	Frequency	E_2^-/E_2^+	Δ	Frequency	B_2^-/A_2^+	Δ
$K_a = 0 \leftarrow 0$									
$4_{04} \leftarrow 5_{05}$	4244069.3	B_2^+	−0.9						
$2_{02} \leftarrow 3_{03}$	4270732.5	B_2^+	−2.36						
$1_{01} \leftarrow 2_{02}$	4283560	A_2^-	3.28						
$0_{00} \leftarrow 1_{01}$	4296051.5	B_2^+	0.95						
$2_{02} \leftarrow 1_{01}$	**4331656.1**	B_2^+	1.32						
$3_{03} \leftarrow 2_{02}$	**4342910.7**	A_2^-	2.1				4270654	B_2^-	0.22
$4_{04} \leftarrow 3_{03}$	**4353850.4**	B_2^+	1.61				4283797.5	A_2^+	−1.82
$5_{05} \leftarrow 4_{04}$							4297008	B_2^-	−2.29
$6_{06} \leftarrow 5_{05}$							4310212.9	A_2^+	−1.38
$7_{07} \leftarrow 6_{06}$							**4323352.7**	B_2^-	−0.3
$9_{09} \leftarrow 8_{08}$							**4349273.7**	B_2^-	0.08
$K_a = 0 \leftarrow 1$									
$8_{08} \leftarrow 9_{18}$	**4159964.53**	B_2^+	−0.6						
$7_{07} \leftarrow 8_{17}$	**4176635.91**	A_2^-	0.94						
$6_{06} \leftarrow 7_{16}$	**4192878.5**	B_2^+	1.22						
$4_{04} \leftarrow 5_{14}$	4223988.5	B_2^+	−2.01	**4195654.3**	E_2^+	−0.67	**4156937**	A_2^+	1.4
$3_{03} \leftarrow 4_{13}$	4238804.5	A_2^-	−2.81				**4169654.1**	B_2^-	2.41
$2_{02} \leftarrow 3_{12}$				4222725.5	E_2^+	1.59	**4182284.5**	A_2^+	−2.1
$1_{01} \leftarrow 2_{11}$	4266803	A_2^-	−0.95	4235876	E_2^-	−1.16	4194867	B_2^-	−1.72
$0_{00} \leftarrow 1_{10}$	4279920	B_2^+	−1.21				4207416	A_2^+	−1.43
$1_{01} \leftarrow 1_{11}$	4292009.5	A_2^-	−0.54	4261185	E_2^-	−0.38	4220134.5	B_2^-	2.49
$2_{02} \leftarrow 2_{12}$	4291200.5	B_2^+	2.71	4261011.5	E_2^+	−0.38	4220497.5	A_2^+	1.66
$3_{03} \leftarrow 3_{13}$	4289989.5	A_2^-	−1.16	4260748.5	E_2^-	0.86	4220979	B_2^-	1.33
$4_{04} \leftarrow 4_{14}$	4288396.5	B_2^+	−3.47	4260387.5	E_2^+	−0.42	4221521.5	A_2^+	−0.23
$5_{05} \leftarrow 5_{15}$	4286439.3	A_2^-	1.27	4259924.7	E_2^-	−1.62	4222073.9	B_2^-	−1.25
$6_{06} \leftarrow 6_{16}$	4284116.1	B_2^+	−0.74				4222592.9	A_2^+	0.03
$7_{07} \leftarrow 7_{17}$	**4281449.12**	A_2^-	1.76				4223039.2	B_2^-	−0.14
$8_{08} \leftarrow 8_{18}$	**4278436.76**	B_2^+	−2.26				4223388.5	A_2^+	−0.39
$11_{011} \leftarrow 11_{111}$	**4267451.44**	A_2^-	0.21						
$2_{02} \leftarrow 1_{10}$	**4315526.4**	B_2^+	0.95	4285299.5	E_2^+	−0.94	4244795.5	A_2^+	−1.41
$3_{03} \leftarrow 2_{11}$	**4326152.1**	A_2^-	−3.72	4296808.5	E_2^-	0.76	4257077	B_2^-	1.59
$4_{04} \leftarrow 3_{12}$	**4336205.1**	B_2^+	1.82	4308009	E_2^+	1.34	4269209.5	A_2^+	−0.3
$5_{05} \leftarrow 4_{13}$	**4345701.5**	A_2^-	2.57	**4318927.7**	E_2^-	1.77	4281175.3	B_2^-	0.64
$6_{06} \leftarrow 5_{14}$				**4329582.4**	E_2^+	0			
$7_{07} \leftarrow 6_{15}$				**4339987.6**	E_2^-	−1.69	4304523.8	B_2^-	3.23
$8_{08} \leftarrow 7_{16}$				**4350152.47**	E_2^+	0.93			
$9_{09} \leftarrow 8_{17}$							**4327013.9**	B_2^-	−0.35
$K_a = 1 \leftarrow 0$									
$4_{13} \leftarrow 5_{05}$	**4267451.44**	B_2^+	0.51						
$3_{12} \leftarrow 4_{04}$	**4279965.56**	A_2^-	−0.92						
$2_{11} \leftarrow 3_{03}$	**4292356.3**	B_2^+	3				**4175234.46**	A_2^+	1.88
$1_{10} \leftarrow 2_{02}$							**4187988.17**	B_2^-	−2.22
$1_{11} \leftarrow 1_{01}$	**4328878.5**	B_2^+	1.92				4212700.6	A_2^+	1.03
$2_{12} \leftarrow 2_{02}$	**4328536.4**	A_2^-	2.1				4212922	B_2^-	−1.18
$3_{13} \leftarrow 3_{03}$	**4328001.1**	B_2^+	2.62				4213220.9	A_2^+	−1.9
$4_{14} \leftarrow 4_{04}$	**4327251.2**	A_2^-	3.39				4213565.9	B_2^-	−1.5
$5_{15} \leftarrow 5_{05}$	**4326258.3**	B_2^+	−2.02				4213927	A_2^+	−0.53
$6_{16} \leftarrow 6_{06}$	**4325015.13**	A_2^-	−0.23				4214277.6	B_2^-	0.2
$7_{17} \leftarrow 7_{07}$	**4323494.7**	B_2^+	0.26				4214594.1	A_2^+	−1.07
$8_{18} \leftarrow 8_{08}$	**4321681.5**	A_2^-	0.14				4214860.4	B_2^-	−1.8
$1_{10} \leftarrow 0_{00}$							**4224436.6**	B_2^-	3.95
$2_{11} \leftarrow 1_{01}$	**4353274.88**	B_2^+	1.65				**4236011.16**	A_2^+	−1.51

(*continued*)

Table 5(a). Continued.

Transition	Frequency	A_2^-/B_2^+	Δ	Frequency	E_2^-/E_2^+	Δ	Frequency	B_2^-/A_2^+	Δ
$K_a = 1 \leftarrow 1$									
$7_{17} \leftarrow 8_{18}$	**4207633.1**	B_2^+	0.94						
$6_{16} \leftarrow 7_{17}$	**4221760.2**	A_2^-	−1.81						
$5_{15} \leftarrow 6_{16}$	**4235623.4**	B_2^+	−0.26						
$3_{13} \leftarrow 4_{14}$	**4262548.6**	B_2^+	−1.06				**4150948.3**	A_2^+	3.1
$2_{12} \leftarrow 3_{13}$	**4275615.2**	A_2^-	−1.17						
$1_{11} \leftarrow 2_{12}$	**4288416.3**	B_2^+	−3.29				**4175540.9**	A_2^+	1.71
$1_{11} \leftarrow 1_{10}$	**4312742.8**	B_2^+	−4.44						
$2_{12} \leftarrow 2_{11}$	**4311778.2**	A_2^-	−3.33				4199342.8	B_2^-	−2.04
$4_{14} \leftarrow 4_{13}$							**4197733.65**	B_2^-	1.88
$5_{15} \leftarrow 5_{14}$	**4306179.9**	B_2^+	−0.78						
$6_{16} \leftarrow 6_{15}$							**4195441.87**	B_2^-	−3.08
$8_{18} \leftarrow 8_{17}$							**4192605.2**	B_2^-	2.41
$2_{12} \leftarrow 1_{11}$	**4336990**	A_2^-	2.38				4224606.5	B_2^-	−1.63
$3_{13} \leftarrow 2_{12}$	**4348463.5**	B_2^+	2.09				4236843.5	A_2^+	1.01
$5_{15} \leftarrow 4_{14}$							4261250.7	A_2^+	1.42
$6_{16} \leftarrow 5_{15}$							**4273414.2**	B_2^-	2.39
$9_{18} \leftarrow 10_{19}$	**4173521.2**	A_2^-	1.61						
$8_{17} \leftarrow 9_{18}$	**4188921.8**	B_2^+	−2.53						
$7_{16} \leftarrow 8_{17}$	**4204005.6**	A_2^-	−2.94						
$6_{15} \leftarrow 7_{16}$	**4218773.5**	B_2^+	−2.68						
$5_{14} \leftarrow 6_{15}$	**4233231.36**	A_2^-	1.31						
$4_{13} \leftarrow 5_{14}$	**4247372.04**	B_2^+	0.76						
$3_{12} \leftarrow 4_{13}$	**4261198.28**	A_2^-	−0.36						
$2_{11} \leftarrow 3_{12}$	**4274707.56**	B_2^+	−0.22				**4160643.07**	A_2^+	0.02
$1_{10} \leftarrow 2_{11}$	**4287891.96**	A_2^-	1.04				**4174409.5**	B_2^-	−2.52
$1_{10} \leftarrow 1_{11}$	**4313093.3**	A_2^-	−3.7						
$2_{11} \leftarrow 2_{12}$	**4312812.9**	B_2^+	−3.3						
$3_{12} \leftarrow 3_{13}$	**4312385.5**	A_2^-	3.52						
$4_{13} \leftarrow 4_{14}$	**4311778.21**	B_2^+	−2.5						
$5_{14} \leftarrow 5_{15}$	**4310996.3**	A_2^-	−0.9						
$6_{15} \leftarrow 6_{16}$	**4310018.38**	A_2^-	2.64						
$7_{16} \leftarrow 7_{17}$	**4308822.5**	B_2^+	1.56						
$8_{17} \leftarrow 8_{18}$	**4307399**	A_2^-	0.78						
$2_{11} \leftarrow 1_{10}$	**4337145.3**	B_2^+	1.41						
$3_{12} \leftarrow 2_{11}$	**4348550**	A_2^-	2.86						

Symmetry label pertains to the ground state.
Δ is the difference between the observed and the calculated transition frequency.
New transitions in bold.

unquestionable A_2/B_2 subbands. While we agree with this reasoning, we would argue that neither the current assignment of the 4261 GHz subband to the $(DT)^2$ $K_a = 0 \leftarrow 1_{(lower)}$ subband nor its assignment to an E_2 $K_a = 1 \leftarrow 1_{(lower)}$ subband is entirely satisfactory, and suggest that assignment to $K_a = 1$ $(E_1) \leftarrow 1$ (E_2) transitions be considered. Verification of the excited state of this subband is therefore critical to its assignment. Presently however, we address the unequivocally assigned A/B subbands and the still non-assigned 4295 GHz E-state Q-branch, since an overview of the subbands observed in this frequency region will aid our discussion of the 4261 GHz subband assignment.

Since Keutsch *et al*. [4] had observed only the lowest frequency subbands of the $K_a = 1 \leftarrow 0$ and $K_a = 1 \leftarrow 1$ bands, their assignment of these transitions as originating in the B_2^-/A_2^+ states relied on the characteristic Coriolis shifts of the ground state $K_a = 0$ energy levels, along with the combination differences of the ground state $K_a = 1$ transitions terminating in the same excited states. We have subsequently observed the higher frequency subbands of the $K_a = 1 \leftarrow 0$ and $K_a = 1 \leftarrow 1$ bands. These subbands were assigned in an analogous manner.

Transitions to the excited state E_2 levels of the $K_a = 1$ stack cannot be precisely predicted for this vibration

Table 5(b). Fitted rotational constants of the $(DT)^2$ and (S) bands of $(H_2O)_2$ (MHz).

		A_2^-/B_2^+	E_2^-/E_2^+	B_2^-/A_2^+
$K_a = 0$	$B^{(0)}$	5999.0 (3)	6094.65 (9)	5982.90 (6)
	$D^{(0)}$	0.529 (5)	0.113 (1)	0.0517 (4)
	$^{()}$	4 271 376.9 (6)[b]		
	$I^{(0)}$	56 276 (1)		
	$\nu_{BT}^{(0)}$	2547.4 (6)[b]		
$K_a = 1$	$B^{(1)}$	6147.5 (2)	n/a	6012.25 (5)
	$D^{(1)}$	0.081 (2)	n/a	0.0769 (7)
	$(B - C)^{(1)}/4$	16.2 (2)	n/a	7.26 (4)
	$d^{(1)}$	0.003 (2)	n/a	−0.0017 (6)
		−3078[a]	n/a	1440[a]
	$^{(1)}$	n/a		
	$I^{(1)}$	96797 (1)		
	$\nu_{BT}^{(1)}$	n/a		

$\sigma_{rms} = 1.86$ MHz.Symmetry labels pertain to excited state.

[a] Fixed.

[b] Dependent on the current assignment of the E_2-states; otherwise not determinable.

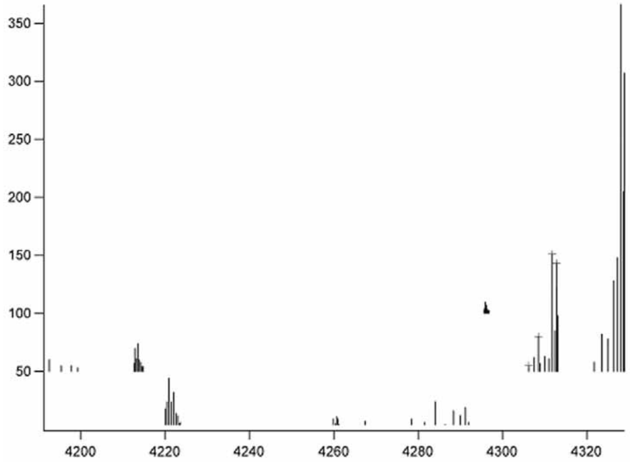

Figure 5. Q-branches of the newly assigned subbands listed in table 5(a). Lower Q-branches correspond to subbands terminating in $K_a = 0$, middle Q-branches correspond to subbands terminating in $K_a = 1$, and upper Q-branch corresponds to lone 4295 GHz Q-branch, which is likely too high in frequency to terminate in $K_a = 1$ E-states of (S).

since the rotational constants necessary for an analytical prediction are not available. It is, however, likely that they will be found near the midpoint of the upper and lower frequency subbands. We now capitalize on knowledge of the upper state energies and more confidently rule out assignment of the 4295 GHz Q-branch observed by Keutsch *et al.* to these levels. Indeed, assignment of the 4295 GHz subband to the E_2 $K_a = 1 \leftarrow 1$ (S) subband would place these states only about 9 GHz below the B_2^-/A_2^+ (S) states, but 88 GHz above the B_2^+/A_2^- (S) states. While this is conceivable by way of an enormous bifurcation splitting, it is extremely unlikely, and Coriolis shifting is not expected to affect the 4295 GHz subband, since it appears free of any perturbation. Figure 5 shows the Q-branches associated with all of the observed subbands mentioned in this section. Figure 6 indicates the relative energy, namely 4306970.87 MHz, of the $J = 1$, $K_a = 1$ level that would result from the assignment of the 4295 GHz subband to the E_2 $K_a = 1 \leftarrow 1$ subband.

Keutsch *et al.* postulated that if the 4295 GHz Q-branch did not belong to the E_2 $K_a = 1 \leftarrow 1$ (S) subband, it undoubtedly corresponded to an E_1 $K_a = 1 \leftarrow 0$ subband of $(DT)^2$. Because these transitions do not alternate in intensity, they are expected to be of E-symmetry (see nuclear spin weights). Furthermore, they appear to be free of any Coriolis perturbations that would otherwise associate them with the ground state 2s of the $K_a = 0$ stack or the upper asymmetry component of the ground state 2s of the $K_a = 1$ stack. Also, vibrational transitions originating in the 1s of the $K_a = 1$ stack have never been observed, presumably because of low thermal populations. These considerations along with general selection rules leave only E_2 $K_a = 1 \leftarrow 1_{(lower)}$ (A′), E_1 $K_a = 1 \leftarrow 0$ (A′ or A″), and E_2 $K_a = 0 \leftarrow 1_{(lower)}$ (A′) as possible assignments, unless $E_2 \leftrightarrow E_1$ transitions are taken into account.

We argued against assigning the 4295 GHz Q-branch to E_2 $K_a = 1 \leftarrow 1_{(lower)}$ (S). Keutsch *et al.* [4] discarded the $K_a = 0 \leftarrow 1_{(lower)}$ option, arguing that this would require the existence of an additional vibrational level. Indeed, Keutsch *et al.* had reassigned the transitions previously associated with the IPB, or $(DT)^2$, $K_a = 0$ stack to DT $E_2 \leftrightarrow E_1$ transitions, as will be discussed in

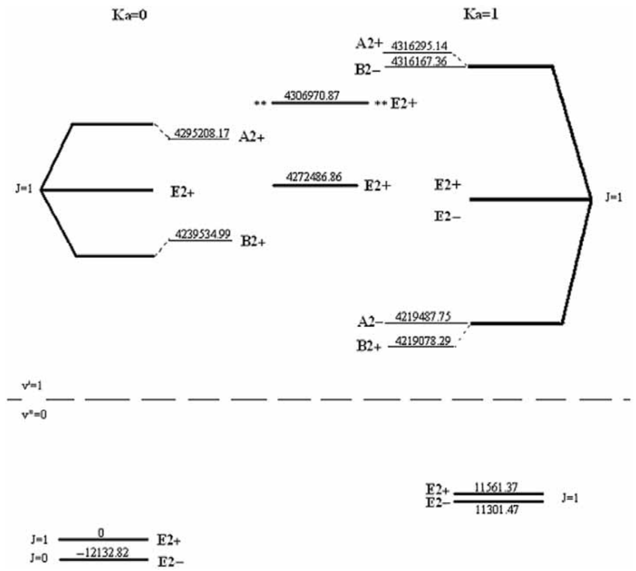

Figure 6. Relative energies of H_2O dimer excited states (MHz). Energies have been calculated relative to the ground state E_2^+ $J=1$, $K_a=0$ level. Coriolis shifts are indicated by dashed lines. The upper asymmetry component (B_2^+) of the excited state $K_a=1$ stack has been shifted lower in energy and is now located below the lower asymmetry component. The energy level at 4272486.86 MHz (transition frequency 4261185 MHz) originates from a state of E_2^- symmetry and therefore terminates in either an E_2^+ or an E_1^+ state, but remains of unconfirmed vibration. The energy level at 4306970.87 MHz is of E-symmetry, but may belong to either the 1s or the 2s, and is also of unknown vibration; the indicated energy corresponds to assignment of the 4295669.4 MHz transition of the 4295 GHz Q-branch to an E_2 subband originating in $K_a = 1_{(\mathrm{lower})}$.

the next section. This led to the assignment of the newly observed transitions to the $K_a=0$ $(\mathrm{DT})^2$ instead of to the hydrogen bond stretch (S) $K_a=0$ stack, which was in better accord with theoretical predictions (table 3(a)) since (S) is predicted at a noticeably higher frequency. The 4295 GHz Q-branch is higher, rather than lower in frequency, however, than the newly assigned $(\mathrm{DT})^2$ subbands. Since the higher frequency $K_a=0$ (S) has not yet been assigned, an additional vibrational level would not be required for a $K_a=0 \leftarrow 1_{(\mathrm{lower})}$ assignment, although agreement between theory and experiment would be poor and no additional A/B transitions have been observed at lower frequencies to indicate the presence of an additional vibrational level. We mentioned in the last section that theory predicts the ordering of vibrational symmetries quite well for the $K_a=0$ stack; however, inspection of the vibrational frequencies reveals calculated values that are often higher, by inconsistent amounts, than those found experimentally. We therefore caution against ruling out a $K_a=0 \leftarrow 1_{(\mathrm{lower})}$ assignment for the 4295 Q-branch transitions as they may correspond to the 2s of (S), though this seems unlikely. Transition frequencies were predicted analytically for the $K_a=0 \leftarrow 0$ subband that would be expected if the excited states of the 4295 GHz Q-branch indeed belonged to the $K_a=0$ stack, but no matches were found. This further discredits a $K_a=0 \leftarrow 1_{(\mathrm{lower})}$ assignment of the 4295 GHz transitions. Concerning a different E_2 $K_a=1 \leftarrow 1_{(\mathrm{lower})}$ assignment, only an A′ vibration higher in frequency than the newly assigned (S) would allow this assignment and none is predicted below $200\,\mathrm{cm}^{-1}$ for the $K_a=1$ stack. Furthermore, an A″ vibration, DT + AW, is expected next.

Finally, we are left to consider the E_1 $K_a=1 \leftarrow 0$ assignment to $(\mathrm{DT})^2$ proposed by Keutsch *et al.* [4] The A_2^-/B_2^+ subband of the $(\mathrm{DT})^2$, previously labelled IPB, has already been assigned and is of confirmed A′ symmetry. Assignment of the 4295 GHz band to the 1s of the $(\mathrm{DT})^2$ would result in an excited state $\mathrm{AS}^{(1)}$ of ~900 GHz, whereas theory predicts a splitting on the order of 300 GHz (*37*). Furthermore, since the 2s of the AW have also been assigned and are of confirmed A′ symmetry, it is unlikely that the vibrational assignment of the $(\mathrm{DT})^2$ 2s is incorrect. While we cannot rule out the $(\mathrm{DT})^2$ E_1 $K_a=1 \leftarrow 0$ assignment based on an enhanced excited state AS splitting, such an assignment will be difficult to verify, since, as mentioned, we do not expect to observe transitions originating from the 1s of the $K_a=1$ stack. While nothing precludes assigning these transitions to an analogous A″ vibration, only A′ vibrations are expected in this frequency region rendering, that option unlikely.

One other possible assignment remains that was not mentioned by Keutsch *et al* [4]. The 4295 GHz Q-branch transitions could correspond to excited $E_2 \leftrightarrow E_1$ transitions. Such an assignment is supported by the lack of any A or B symmetry components that would otherwise be expected to occur higher and lower in frequency than the E-state components. Aside from a few GHz centred on the 70 μm FIR laser line, the region surrounding this lone Q-branch has been scanned meticulously from 148 GHz lower in frequency to 60 GHz higher in frequency. Recall, however, that the nuclear spin weights of the A_2 and B_2 states are equal to/double that of the E_2 states, while the nuclear spin weights of the A_1 and B_1 states are three times less than/null compared to that of the E_1 states. These weights support the $(\mathrm{DT})^2$ E_1 $K_a=1 \leftarrow 0$ assignment proposed by Keutsch *et al.* regardless of other symmetry components having been observed, while further disfavoring an E_2 $K_a=0 \leftarrow 1_{(\mathrm{lower})}$ (S) assignment. The frequencies of the lone E-state subband are listed in table 6. Clearly, additional information including scanning at higher

Table 6. Lone Q-branch transitions (MHz).

Q(1)	4295669.4
Q(2)	4295723.5
Q(3)	4295801.6
Q(4)	4295903.5
Q(5)	4296032.7
Q(6)	4296187.8
Q(7)	4296368.5
Q(8)	4296572.2

frequencies is required before these transitions may be assigned.

All $(H_2O)_2$ water dimer transitions were fit according to the equations of [4]. In addition to the Coriolis term that Keutsch *et al.* introduced for the excited state A_2^-/B_2^+ energy levels, a Coriolis term was required for the B_2^-/A_2^+ energy levels. This reinforces association of these energy levels with the same vibration. The Coriolis term for the latter is, however, over twice as large as that of the former, which is indicative of a much greater perturbation. Inspection of the relative energies (figure 6) of the upper and lower asymmetry components of the A_2^-/B_2^+ energy levels reveals that the upper asymmetry components have been shifted lower in energy, so much that they are located lower in energy than the lower asymmetry components. The Coriolis term that we report here for the B_2^-/A_2^+ energy levels is, in contrast, positive, indicating that these energy levels of the $K_a = 1$ stack have been shifted to higher energies, because they are higher in energy than their perturbers, notably the energy levels of the $K_a = 0$ stack.

The Coriolis shifts indicated in figure 6 are on the order of tens to hundreds of MHz. The asymmetry components of the $K_a = 1$ B_2^-/A_2^+ levels for example, were shifted further apart, and are now split by 128 MHz; their ordering did not change. The pre-shifted separation between these asymmetry components would consequently have been between zero and 128 MHz. Therefore, an unperturbed energy separation of roughly 20900 MHz resulted in this Coriolis shift. In comparison, the forks of the $K_a = 0$ and 1 vibrations are centred at nearly the same energies, and we expect the E_2-states of the $K_a = 0$ and 1 stacks to be exceedingly close in energy, perhaps separated by as little as 1000 MHz. Therefore, it is expected that the E_2-states undergo much larger Coriolis shifts than the A/B-states. As mentioned earlier, the E-states of a given fork are expected to be located approximately halfway between the upper and lower A/B prongs. For example, the unperturbed E-states of the $(D_2O)_2$ DT $K_a = 0$ stack are off-centre by only 37 MHz for the 1s and 11 MHz for the 2s. This approximation is therefore a good one.

The energy level expression we use pertaining to Coriolis perturbed pairs is

$$E = \frac{[E^{(0)} + E^{(1)}]}{2} \pm \left[\frac{(E^{(1)} - E^{(0)})^2}{4} + \frac{\zeta^2 J(J+1)}{2}\right]^{1/2} \quad (8)$$

where $E^{(n)}$ represents the energies of the unperturbed levels and ζ is the Coriolis interaction constant. In the limit that $E^{(0)}$ approaches $E^{(1)}$, the Coriolis shift becomes almost exclusively J-dependent. Furthermore, the Coriolis interaction constant must be increased in magnitude as the energy levels are brought closer together in order to account for the increasing perturbation of the levels. A Coriolis interaction constant on the order of 10 GHz is expected to be necessary to account for the perturbations resulting when energy levels are separated by ~1000 MHz. This would effectively destroy our two strongest Q-branch identifying tools, the constant second difference and the compact nature of the transitions. For this reason, it may be quite difficult to identify these highly perturbed Q-branches associated with the E_2-states of the $K_a = 0$ and 1 stacks. Instead, the P- and R-branch transitions corresponding to the $K_a = 0 \leftarrow 0$ subband should be searched for based on ground state combination differences which are not affected by such perturbations. Once they are located, the $K_a = 0 \leftarrow 1$ E_2-state Q-branch can be analytically predicted and the Coriolis shift estimated.

Such an unprecedentedly large Coriolis perturbation effectively explains the non-observation of the subbands associated with the $K_a = 0$ E_2-states and the upper asymmetry component of the $K_a = 1$ E_2-states. However, we are left with two unperturbed and unassigned E-state Q-branches at 4295 and 4261 GHz (figure 6), two E_2-state energy levels supposed to be highly perturbed, and one unperturbed E_2-state energy level (lower asymmetry components of the $K_a = 1$ E_2-states). Unfortunately, neither of the observed Q-branches is easily attributed to any of these energy levels. First, both the 4295 GHz and the 4261 GHz E-state Q-branches are well behaved, showing nearly perfect constant second differences. Furthermore, they are quite compact. This makes it highly unlikely that they would correspond to the severely Coriolis-perturbed states discussed above. Second, we have shown that unperturbed E-states are expected to be very nearly centered between the upper and lower prongs of the vibrational fork. The most 'well-centred' E-state Q-branch, still off-centre by 4.7 GHz, is of course that at 4261 GHz assigned by Keutsch *et al.* [4] to the $K_a = 0 \leftarrow 1$ $(DT)^2$ subband. The 4261 GHz Q-branch clearly originates, however, in $K_a = 1_{(lower)}$ E_2 ground states, and is therefore not of the correct symmetry to be assigned to the unperturbed lower asymmetry component of the excited $K_a = 1$ E-states. Therefore, we conclude that the 4261GHz Q-branch does not belong to either the assigned $(DT)^2$ $K_a = 0$ vibration, nor to the (S) $K_a = 1$ vibration. Since this subband necessarily corresponds to either $K_a = 0 \leftarrow 1_{(lower)}$ or $K_a = 1 \leftarrow 1_{(lower)}$ of an A′ vibration originating in the 2s, and the current analysis leaves no unaccounted for $K_a = 1$ A′ vibrations, this subband may correspond to $K_a = 1$ $(E_1) \leftarrow 1$ (E_2) transitions terminating in the $K_a = 1$ stack of (S), in which case a P(1) transition would not be expected.

A satisfactory assignment of the 4261 GHz transitions will not be obtained until the nature of the excited state is elucidated. Similarly, the 4295 GHz Q-branch cannot be confidently assigned. Based on previous arguments along with those just discussed, we concluded that it most likely corresponds not to an E_2 subband, but rather to the $(DT)^2$ E_1 $K_a = 1 \leftarrow 0$ subband. The P- and R-branches associated with the 4295 GHz Q-branch should be searched for as they would allow the calculation of combination differences useful in assigning the ground state.

4.3. *Excited state E_1 ($K_a = 0$) ← E_2 ($K_a = 1$) transitions in the $(H_2O)_2$ water dimer*

As mentioned in the previous section, Keutsch *et al.* reassigned the transitions previously associated with the IPB $K_a = 0$ stack to DT $E_1 \leftarrow E_2$ transitions and the $K_a = 1$ stack to the $(DT)^2$ [4, 11]. The reassignment of the latter represents only a change in vibrational labelling, so that these transitions are now labelled according to the scheme of Smit *et al.* [17] The reassignment of the former, in contrast, revolutionized the way spectroscopists approach E-state subbands

Harker *et al.* [3] recently examined in great detail the theory surrounding $E_2 \leftrightarrow E_1$ transitions and how they had come to be thought of as weak and experimentally inaccessible [21]. We refer the reader to this article, and review here only the essential details: (1) the labelling of E-states with 1s and 2s is purely a matter of convenience and does not affect the selection rules governing these states; (2) transitions between E-states are allowed as long as the rule $+ \leftrightarrow -$ is respected; (3) recent theoretical works predict dipole moments for $E_2 \leftrightarrow E_1$ transitions that are accessible with current experimental design; (4) $E_2 \leftrightarrow E_1$ transitions allow us to link two otherwise disjointed sets of transitions and thereby to experimentally determine tunneling splittings essential to the establishment of a universal water potential energy surface (PES).

During the analysis of the $(H_2O)_2$ donor torsion overtone $(DT)^2$ and stretch (S) vibrations presented in the previous section, Keutsch *et al.* [4] consulted theoretical predictions of the transition dipole moments for select excited state water dimer transitions. Surprisingly, $E_1 \leftarrow E_2$ transitions to the $K_a = 0$ stack of the donor torsion were predicted to be comparable in strength to the regular ($E_2 \leftrightarrow E_2$, $E_1 \leftrightarrow E_1$) transitions assigned to the $(DT)^2$ and (S). Interestingly, the transitions that Braly *et al.* had assigned to the $K_a = 0$ stack of the in-plane bend (IPB) vibration,[11] while in very poor agreement with the $K_a = 0$ energy levels predicted by the three most sophisticated theoretical potentials available [16, 17, 22] were in much better agreement with $E_1 \leftarrow E_2$ transitions to the $K_a = 0$ stack of the donor torsion. Furthermore, no A or B components that would be expected near regular E-state transitions had been observed despite exhaustive scanning of the spectral region. Lastly, Keutsch *et al.* [4] recently observed A′ transitions terminating in the $K_a = 0$ stack that coincided much better with theoretical predictions for the $(DT)^2$ than did the 'IPB' transitions. We mention also that, in accord with the last section, we have reason to believe that we observed the first of the $K_a = 0$ (S) subbands. Such an assignment would not be conceivable were the $K_a = 0$ 'IPB' transitions instead assigned to the $(DT)^2$, since the transitions currently assigned to the $(DT)^2$ would then necessarily be assigned to the (S).

In order to support this novel assignment, Keutsch *et al.* [4] needed to establish that the transitions originated in the lower asymmetry component E_2-states of the $K_a = 1$ stack and terminated in the $K_a = 0$ stack. Indeed, only A″ vibrational levels were predicted in the correct energy range once the $(DT)^2$ and even higher frequency (S) were ruled out as possible assignments. If the transitions originated in the upper asymmetry component E_2-states, they could be attributed to regular A″ transitions. On the other hand, if they did not terminate in the $K_a = 0$ stack, they could be attributed to the $K_a = 1$ (S) for which other transitions in better accord with theory had already been observed. However, transitions that originated in the lower asymmetry component E_2-states and terminated in the $K_a = 0$ stack could terminate in the E_1-states of an A″ vibration such as the (DT).

Keutsch *et al.* [4] used ground state combination differences and characteristic Coriolis shifts to establish that the IPB transitions originated in the lower asymmetry component of the $K_a = 1$ E_2-states. Unequivocally establishing a $K_a = 0$ excited state was not as easily done. While the $K_a = 0 \leftarrow 1$ subband sported a P(1) transition unique to excited state $K_a = 0$ stacks, the $K_a = 0 \leftarrow 0$ subband that apparently terminated in the same excited states was comprised of only one transition, namely R(1). Whereas a better established $K_a = 0 \leftarrow 0$ subband would have conclusively

Table 7(a). $E_1 \leftarrow E_2$ transitions terminating in the (DT) $K_a = 0$ stack of H_2O (MHz).

Transition	Frequency	E_2^-/E_2^+	Δ
$K_a = 0 \leftarrow 0$			
$4_{04} \leftarrow 5_{05}$	**3 036 009.00**	E_2^+	−3.39
$303 \leftarrow 4_{04}$	**3 046 921.40**	E_{2-}	1.11
$2_{02} \leftarrow 3_{03}$	**3 058 089.80**	E_2^+	0.09
$1_{01} \leftarrow 2_{02}$	**3 069 547.10**	E_{2-}	−1.58
$0_{00} \leftarrow 1_{01}$	**3 081 330.80**	E_2^+	1.42
$2_{02} \leftarrow 1_{01}$	3 118 839.0	E_2^+	0.74
$K_a = 0 \leftarrow 1$			
$2_{02} \leftarrow 3_{12}$	**3 044 701.20**	E_2^+	0.03
$1_{01} \leftarrow 2_{11}$	3 057 223.1	E_2^-	−0.24
$0_{00} \leftarrow 1_{10}$	3 069 767.2	E_2^+	−0.81
$1_{01} \leftarrow 1_{11}$	3 082 529.0	E_2^-	−2.57
$2_{02} \leftarrow 2_{12}$	3 082 991.0	E_2^+	1.87
$3_{03} \leftarrow 3_{13}$	3 083 678.8	E_2^-	−0.7
$4_{04} \leftarrow 4_{14}$	3 084 586.6	E_2^+	1.21
$5_{05} \leftarrow 5_{15}$	3 085 730.0	E_2^-	0.03
$6_{06} \leftarrow 6_{16}$	3 087 095.0	E_2^+	−0.38
$7_{07} \leftarrow 7_{17}$	3 088 689.0	E_2^-	−0.46
$8_{08} \leftarrow 8_{18}$	**3 090 507.30**	E_2^+	−0.48
$9_{09} \leftarrow 9_{19}$	**3 092 546.20**	E_2^-	−1.94
$10_{010} \leftarrow 10_{110}$	**3 094 811.00**	E_2^+	0.9
$11_{011} \leftarrow 11_{111}$	**3 097 293.10**	E_2^-	1.06
$12_{012} \leftarrow 12_{112}$	**3 099 991.70**	E_2^+	−0.48
$3_{03} \leftarrow 2_{11}$	3 119 735.4	E_2^-	0.24
$4_{04} \leftarrow 3_{12}$	3 132 209.2	E_2^+	56
$5_{05} \leftarrow 4_{13}$	**3 144 732.80**	E_2^-	3.25
$6_{06} \leftarrow 5_{14}$	3 157 327.1	E_2^+	−0.22
$7_{07} \leftarrow 6_{15}$	**3 170 015.60**	E_2^-	0.11

Symmetry label pertains to the ground state.
Δ is the difference between the observed and the calculated transition frequency.

Table 7(b). Fitted rotational constants of the $(H_2O)_2$ (DT) (MHz).

		A_1^+/B_1^-	E_1^+/E_1^-	B_1^+/A_1^-
$K_a = 0$	$B^{(0)}$	n/a	6251.94 (2)	n/a
	$D^{(0)}$	n/a	0.0540 (2)	n/a
	$^{()}$	3 094 955.7 (5)[a]		
	$I^{(0)}$	n/a		
	$\nu_{BT}^{(0)}$	n/a		

[a]Value relative to the $K_a = 0$ ground state of the 2s.
$\sigma_{rms} = 1.35$ MHz.
Symmetry labels pertain to excited state.

established the excited state K_a value, this sparse subband created an ambiguity. Clearly, if the observed P(1) transition were not merely a coincidence and the transitions did indeed terminate in $K_a = 0$, then the analytically predictable $K_a = 0 \leftarrow 0$ subband should be readily identifiable, especially given the extensive scanning efforts devoted to this spectral range. The establishment of the $K_a = 0 \leftarrow 0$ subband assignment as well as the reinforcement of the $K_a = 0 \leftarrow 1$ subband assignment represents our contribution to this novel assignment. We would also like to emphasize that while some of these transitions were identified by extending the scanned spectral region, some of them also came from careful compilation of previously recorded transitions. The transitions originally reported by Braly *et al.* [11] are listed in table 7(a) along with the additional transitions (bold) we observed. Table 7(b) lists the fitted rotational constants.

The assignment of the (DT) $E_1 \leftarrow E_2$ transitions inspired us to calculate the fingerprint of the ground state $E_2 \leftrightarrow E_1$ transitions.[3] The ground state $(H_2O)_2$ $AS^{(0)}$ has been estimated at ~280 GHz using the Local IAM model of Coudert and Hougen [13, 23]. One would therefore expect to observe regular E_1 (DT) transitions to the same $K_a = 0$ stack at frequencies lower by roughly this amount, nominally around 2814 GHz. Identification of these transitions would definitively establish both the ground state AS splitting of $(H_2O)_2$ as well as the feasibility of observing $E_2 \leftrightarrow E_1$ transitions.

5. Conclusions

We have demonstrated the utility of employing a global fitting strategy for assigning the complex VRT spectra of the water dimer by the identification and analysis of all six asymmetry components of a new 'DT' band. This band was used to exemplify why a reassessment of the vibrational assignments within the $K_a = 1$ stacks of both $(H_2O)_2$ and $(D_2O)_2$ is necessary. We extended and clarified existing analyses of the $(H_2O)_2$ donor torsion overtone $(DT)^2$ and the hydrogen bond stretch (S) [4] by augmenting existing subbands, as well as by identifying and assigning four new S subbands. The more complete description of these two vibrations led us to predict Coriolis effects of unprecedented magnitude for two of the three E-states associated with these vibrations and to revise the vibrational assignment of the DT E-states made by Keutsch *et al.* [4]. Finally, we reinforced K_a stack assignments pertaining to the proposal of Keutsch *et al.* [4] that E_1 $(K_a = 0) \leftarrow E_2$ $(K_a = 1)$ have been observed in the vibrationally excited H_2O water dimer. We also demonstrated how the $(H_2O)_2$ ground state AS splittings can be extracted from excited state VRT data.

Comprehensive global fitting is clearly necessary in order to further extend the definitive assignment of the excited state water dimer data set. The spectra of the 1s and 2s can be effectively merged through precise determination of the ground state AS splittings. From these, excited state splittings can be calculated and their dynamical information evaluated, vibrational assignments clarified, and agreement between theory and experiment properly assessed. We identified six new $(D_2O)_2$ (DT) subbands and completed the assignment of the critical $K_a = 0 \leftarrow 0$ $(H_2O)_2$ (DT) subband using this approach.

Acknowledgments

This work was supported by the Experimental Physical Chemistry Program of the National Science Foundation.

References

[1] F. N. Keutsch and R. J. Saykally, Inaugural article: water clusters: untangling the mysteries of the liquid, one molecule at a time. Proceedings of the National Academy of Sciences **98**(19), 10533 (2001).
[2] R. Bukowski, K. Szalewicz, G. C. Groenenboom, and A. V. D. Avoird, J. Chem. Phys. **125,** 044301 (2006).
[3] H. A. Harker, F. N. Keutsch, C. Leforestier, Y. Scribano, J.-X. Han, and R. J. Saykally, Mol. Phys. **105**(5–7), 525 (2006).
[4] F. N. Keutsch, L. B. Braly, M. G. Brown, H. A. Harker, P. B. Petersen, C. Leforestier, and R. J. Saykally, J. Chem. Phys. **119**(17), 8927 (2003).
[5] T. R. Dyke and J.S. Muenter, J. Chem. Phys. **60,** 2929 (1974).
[6] T. R. Dyke, J. Chem. Phys. **66,** 492 (1977).
[7] T. R. Dyke, K. M. Mack, and J. S. Muenter, J. Chem. Phys. **66,** 498 (1977).
[8] J. T. Hougen, J. Mol. Spectrosc. **114**(2), 395 (1985).
[9] L. H. Coudert and J. T. Hougen, J. Mol. Spectrosc. **130,** 86 (1988).
[10] G. T. Fraser, Int. Rev. Phys. Chem. **10,** 189 (1991).
[11] L. B. Braly, J. D. Cruzan, K. Liu, R. S. Fellers, and R. J. Saykally, J. Chem. Phys. **112**(23), 10314 (2000).
[12] L. B. Braly, K. Liu, M. G. Brown, F. N. Keutsch, R. S. Fellers, and R. J. Saykally, J. Chem. Phys. **112**(23), 10293 (2000).
[13] L. H. Coudert and J. T. Hougen, J. Mol. Spectrosc. **139,** 259 (1990).
[14] D. J. Wales, Adv. Mol. Vibrat. Collision Dynam. **3,** 365 (1998).
[15] J. R. Reimer and R. O. Watts, Chem. Phys. **85,** 83 (1984).
[16] C. Leforestier, F. Gatti, R. S. Fellers, and R. J. Saykally, J. Chem. Phys. **117,** 8710 (2002).
[17] M. J. Smit, G. C. Groenenboom, P. E. S. Wormer, and A. V. D. Avoird, J. Phys. Chem. **105,** 6212 (2001).
[18] G. A. Blake, K. B. Laughlin, R. C. Cohen, K. L. Busarow, D.-H. Gwo, C. A. Schmuttenmaer, D. W. Steyert, and R. J. Saykally, Rev. Sci. Instrum. **62**(7), 1693 (1991).
[19] G. A. Blake, K. B. Laughlin, R. C. Cohen, K. L. Busarow, D.-H. Gwo, C. A. Schmuttenmaer, D. W. Steyert, and R. J. Saykally, Rev. Sci. Instrum. **62**(7), 1701 (1991).
[20] N. Goldman, R. S. Fellers, M. G. Brown, L. B. Braly, C. J. Keoshian, C. Leforestier, and R. J. Saykally, J. Chem. Phys. **116,** 10148 (2002).
[21] G. T. Fraser, L. H. Suenram, and L. H. Coudert, J. Chem. Phys. **90,** 6077 (1989).
[22] N. Goldman and R. J. Saykally, J. Chem. Phys. **120,** 4777 (2004).
[23] E. Zwart, J. J. Ter Meulen, W. L. Meerts, and L. H. Coudert, J. Mol. Spectrosc. **147,** 27 (1991).